Femtosecond Plasma Mediated Laser Ablation Has Advantages Over Mechanical Osteotomy of Cranial Bone

David D. Lo, MD,[1] Mark A. Mackanos, PhD,[2,5] Michael T. Chung, BS,[1] Jeong S. Hyun, MD,[1] Daniel T. Montoro, BS,[1] Monica Grova, BS,[1] Chunjun Liu, MD,[1] Jenny Wang, BS,[2] Daniel Palanker, PhD,[2] Andrew J. Connolly, MD, PhD,[3] Michael T. Longaker, MD, MBA,[1,4] Christopher H. Contag, PhD,[2,5,6]* and Derrick C. Wan, MD[1]**

[1]*Hagey Laboratory for Pediatric Regenerative Medicine, Department of Surgery, Plastic and Reconstructive Surgery Division, Stanford University School of Medicine, Stanford, California*
[2]*Hansen Experimental Physics Laboratory, Stanford University, Stanford, California*
[3]*Department of Pathology, Stanford University School of Medicine, Stanford, California*
[4]*Institute for Stem Cell Biology and Regenerative Medicine, Stanford University, Stanford, California*
[5]*Molecular Imaging Program at Stanford, Stanford Center for Photomedicine, Stanford, California*
[6]*Departments of Pediatrics, Radiology, and Microbiology & Immunology, Stanford University School of Medicine, Stanford, California*

Background: Although mechanical osteotomies are frequently made on the craniofacial skeleton, collateral thermal, and mechanical trauma to adjacent bone tissue causes cell death and may delay healing. The present study evaluated the use of plasma-mediated laser ablation using a femtosecond laser to circumvent thermal damage and improve bone regeneration.

Methods: Critical-size circular calvarial defects were created with a trephine drill bit or with a Ti:Sapphire femtosecond pulsed laser. Healing was followed using micro-CT scans for 8 weeks. Calvaria were also harvested at various time points for histological analysis. Finally, scanning electron microscopy was used to analyze the microstructure of bone tissue treated with the Ti:Sapphire laser, and compared to that treated with the trephine bur.

Results: Laser-created defects healed significantly faster than those created mechanically at 2, 4, and 6 weeks post-surgery. However, at 8 weeks post-surgery, there was no significant difference. In the drill osteotomy treatment group, empty osteocyte lacunae were seen to extend 699 ± 27 μm away from the edge of the defect. In marked contrast, empty osteocyte lacunae were seen to extend only 182 ± 22 μm away from the edge of the laser-created craters. Significantly less ossification and formation of irregular woven bone was noted on histological analysis for drill defects.

Conclusions: We demonstrate accelerated bone healing after femtosecond laser ablation in a calvarial defect model compared to traditional mechanical drilling techniques. Improved rates of early regeneration make plasma-mediated ablation of the craniofacial skeleton advantageous for applications to osteotomy. Lasers Surg. Med. 44:805–814, 2012. © 2012 Wiley Periodicals, Inc.

Key words: laser osteotomy; drill osteotomy; Ti:Sapphire laser; plasma-mediated ablation; thermal osteonecrosis

INTRODUCTION

Craniofacial defects due to congenital anomalies, trauma, and tumor resections pose complex challenges in reconstructive procedures of the craniofacial skeleton. Many of these clinical situations require controlled cutting, excising, or surgical remodeling of bony elements [1,2]. Osteotomies fashioned with oscillating saws and drills using carbide or diamond cutting burs are the standard of care. However, the friction from cutting and grinding can cause significant thermal and mechanical trauma to adjacent bone tissue, leading to cell death and delayed healing [3,4]. In addition, mechanical instruments may be difficult to control, making fine, intricate, nonlinear cuts problematic. While the aim is to leave behind a cut edge that is well-suited for early cell attachment, extracellular matrix deposition, and tissue regeneration, use of mechanical instruments may yield a micro-environment suboptimal for bone regeneration.

Recently, endoscopic surgery with an ultrasonic bone cutter (Sonopet Omni®, Synergetics Inc., St. Charles,

All authors have completed and submitted the ICMJE Form for Disclosure of Potential Conflicts of Interest and none were reported.

David D. Lo and Mark A. Mackanos contributed equally to this work.

None of the authors have a financial interest in any of the products, devices, or drugs mentioned in this manuscript.

*Corresponding to: Christopher H. Contag, PhD, Hagey Laboratory for Pediatric Regenerative Medicine, Stanford University School of Medicine, 257 Campus Drive, Stanford University, Stanford, CA 94305-5148. E-mail: ccontag@stanford.edu

**Corresponding author: Derrick C. Wan, MD, Department of Pediatrics, Stanford University School of Medicine, Clark Center E-150, 318 Campus Drive, Stanford, CA 94305-5427.
E-mail: dwan@stanford.edu

Accepted 24 October 2012
Published online 26 November 2012 in Wiley Online Library (wileyonlinelibrary.com).
DOI 10.1002/lsm.22098

MO) has been shown to prevent some of the traditional complications of scarring and intraoperative hemorrhage [5]. However, while this technique minimizes injury to adjacent soft tissue, there is still a potential for collateral damage to cells bordering the osteotomy site [6,7]. Lasers present another alternative for tissue cutting, but can cause osseous tissue damage through photothermal, photoacoustic, photochemical, or photomechanical effects. While carbon dioxide (CO_2) lasers, or other gas or solid-state lasers, have been successful at reducing mechanical friction, they have also been shown to have detrimental effects on healing [8–12]. Lasers with mid-infrared wavelengths, between 2.9 and 10.6 μm, have been evaluated for ablation on skin, aorta, femur, dentin, alveolar bone, cortical bone, and the skull. Importantly, thermal damage still occurs as a consequence of the tissue heating by the laser radiation absorbed in the target tissue [13–17]. Laser ablation aimed at correction of craniosynostosis using neodymium:yttrium-aluminum-garnet (Nd:YAG) and CO_2 lasers also resulted in reduction of the bone regeneration rates due to degenerative changes from thermal damage [18]. Of note, short pulse lasers, such as 10 microsecond CO_2 were shown tro emove dentin with only ~8 μm of thermal damage [19].

In contrast to the linear absorption of the laser radiation by the tissue, plasma-mediated ablation occurs in the focus of the laser beam when ultrashort pulses of high energy are applied. High electric field in the focal area results in ionization of the molecules and formation of plasma, leading to local absorption of the laser radiation, which allows heating the tissue by several thousand degrees during a single pulse. Due to the extremely short interaction time, plasma-mediated laser ablation results in minimal heat diffusion, and consequently, minimal collateral thermal damage. Plasma-mediated laser ablation has already been applied to dermis, cornea, blood vessels, brain, dentin, and bone [20–30]. Previous studies have shown that thermal damage to tissue resulting from plasma-mediated laser ablation can be below a single cell size (<0.2–3.0 μm) [24,31–33]. Since thermal damage is believed to be the most harmful side effect of laser ablation, the purpose of the present study was to therefore compare bone regeneration in calvarial defects created by a femtosecond titanium:sapphire (Ti:Sapphire) laser and conventional drill osteotomies.

MATERIALS AND METHODS

Laser System

The Ti:Sapphire femtosecond laser system (Tsunami, Spectra Physics, Santa Clara, CA) used in this study was tuned to 800 nm wavelength. Pulse duration was 150 femtosecond and repetition rate was set at 1 kHz. The pulse energy was measured with an Ophir Laser Star meter and a PE10-S detector (Ophir Optronics Ltd., Jerusalem, Israel). The average pulse energy was determined by measuring the output power at 1 kHz over an integration period of several seconds. Laser osteotomies were performed with an average pulse energy of 280 μJ. The beam was steered with dielectric mirrors and passed through a 55 mm focal length lens to focus onto the cranial surface into a minimum spot size of ~10 μm, as calculated based on Gaussian beam transformations. The laser was scanned with a two-axis scanning mirror (OIM100 Series, Optics in Motion, Long Beach, CA). A 4-mm diameter circular defect was made with a scanning speed of 4 mm/second. The mirror rotated at one revolution per second while the anesthetized mouse was kept stationary on a platform and required one rotation to ablate the entire depth of the cranium. The Ti:Sapphire laser was coaligned with a helium–neon (HeNe) laser operating at 632.8 nm for visual targeting. Since the mouse was kept stationary, there was no need for dynamic adjustment of the beam position and focusing.

Surgical Procedures

All experiments were performed in accordance with the Stanford University Animal Care and Use Committee guidelines. Fifty-six-day-old wild-type CD1 mice were purchased from Charles River Laboratories (Wilmington, MA). Mice were housed in a light- and temperature-controlled environment and were given food and water *ad libitum*.

For all surgical procedures, the mice were anesthetized with 7.5 mg/kg ketamine, 0.24 mg/kg acepromazine, and 1.5 mg/kg xylazine through an intraperitoneal injection. Under a dissecting microscope (Zeiss, Wetzlar, Germany), the surgical site was cleaned with ethanol, and an incision was made just off the sagittal midline to expose the calvaria. Periosteal tissue was removed and 4-mm calvarial defects were made in nonsuture-associated right parietal bone (~700 μm thick) with the laser ($n = 7$) or with a motorized 200 Series rotary tool (Dremel; Robert Bosch Tool, Racine, WI) using a 4-mm diamond-coated core drill bit ($n = 7$). To minimize thermal injury, all drill defects were performed with constant saline irrigation to minimize thermal injury. In one additional mouse, critical size calvarial defects were created bilaterally. The laser was used to create a 4-mm calvarial defect in the right parietal bone, and the trephine drill bit was used to create a 4-mm calvarial defect in the left parietal bone. Because the dura mater has been shown to be critical for calvarial reossification, a circular piece of expanded polytetrafluoroethylene (ePTFE) surgical membrane (Gore-Tex; W.L. Gore & Associates, Inc., Flagstaff, AZ) was placed into the defect to function as a barrier between the dura and the edges of the bone defect (Fig. 1A) [34]. Incisions were closed using 6–0 Vicryl sutures (Ethicon, Cornelia, GA), and the mice were kept under a warm lamp to maintain their internal temperature until awakening following the anesthesia. No wound infections developed in the animals. Following surgery, mice were kept for up to 8 weeks for micro-CT analysis. At the end of the eighth week and following the last CT scan, the mice were euthanized for histological analysis.

Micro-CT Imaging Analysis

For micro-CT scans, the mice were anesthetized with isoflurane. Imaging was performed using a Siemens

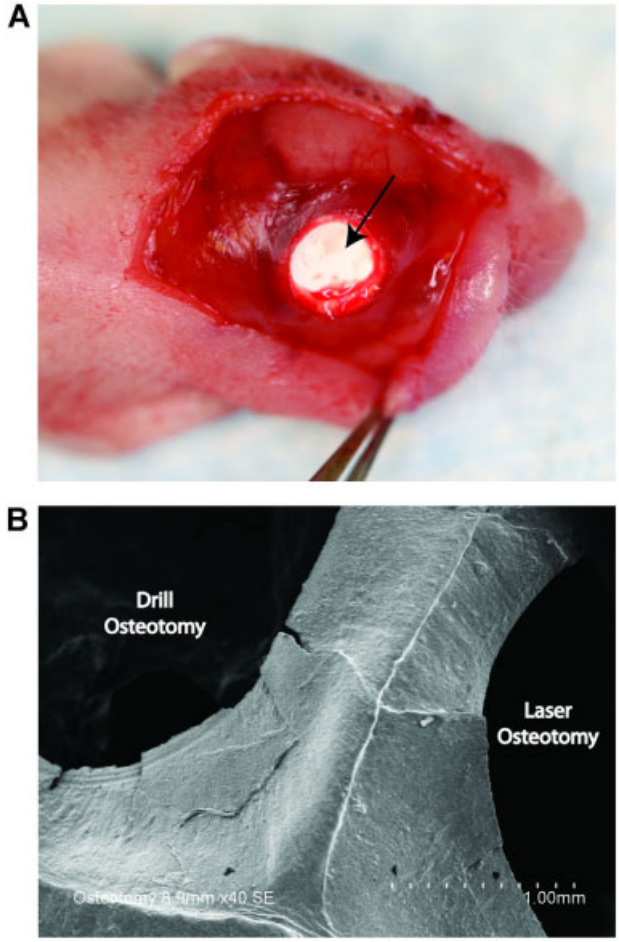

Fig. 1. **A**: Following creation of the calvarial defect, a Gore-Tex membrane (arrow) was placed between the dura mater and the parietal bone in the bone defect to block the contribution of dura mater to newly formed bone. **B**: Scanning electron microscopy (SEM) image taken immediately postoperatively revealed areas of microfractures on the edges of the calvarial defect created by conventional drill osteotomy.

Inveon MicroPET/CT scanner (Siemens Medical Solutions, Inc., Malvern, PA). Using our scan protocol parameters, each image with a 100 μm resolution was acquired in a total scan time of 10 minutes. Mice were scanned immediately postoperatively and at 2, 4, 6, and 8 weeks following surgery. Data were reconstructed into three-dimensional surfaces using the Siemens Inveon Research Workplace 4.0 Software (Siemens Medical Solutions, Inc.).

The three-dimensional reconstructed images were then analyzed using Image J software (Image Processing and Analysis in Java, NIH, Bethesda, MD). The area of the calvarial defects was evaluated by quantifying pixels in the defect. The healing percentage was then determined by dividing the defect area by the defect size immediately postoperatively.

Scanning Electron Microscopic Analysis

Immediately postoperatively, the one mouse with bilateral calvarial defects was euthanized for a qualitative comparison of microstructural changes to bone caused by the femtosecond laser and the mechanical drill bit. After the skull was harvested, the specimen was fixed in 10% phosphate-buffered formalin for 24 hours. After primary fixation, the sample was rinsed in phosphate-buffered saline and dehydrated in an ascending ethanol series (70%, 95%, and 100% for 30 minutes each). The sample was mounted on adhesive carbon film on 15-mm aluminum stubs and sputter coated with 100 Å gold/palladium using a Denton Desk 11 TSC sputter coater (Denton Vacuum, LLC, Moorestown, NJ). Visualization was carried out with a Hitachi S-3400N variable pressure-scanning electron microscope (VP-SEM; Hitachi Ltd., Pleasonton, CA) operated under high vacuum at 10 kV and at a working distance of 6–8 mm.

Histological Analysis

At 3 days and 8 weeks postoperatively, one mouse from each experimental group was chosen to be euthanized for morphological and histological assessment. Skulls were harvested and immediately fixed in 10% formalin overnight, decalcified in 19% EDTA, dehydrated through an ethanol series, and embedded in paraffin as previously described [34]. Eight micrometer-thick coronal sections were cut and collected on Superfrost-Plus slides (Thermo Fischer Scientific, Waltham, MA). For the 3-day time point, sections were prepared and stained with hematoxylin and eosin (H&E), which allowed us to assess the local extent of osteocyte death by displaying osteocyte-occupied lacunae (stained) and empty osteocyte lacunae (unstained). The effects of thermal damage from both the laser osteotomy and drill osteotomy were quantified by measuring the distance the empty osteocyte lacunae extended from the edge of the calvarial defect. Multiple sections were evaluated, and measurements were made in triplicate.

For the 8-week time point, new bone formation was assessed by aniline blue and Movat's pentachrome staining. Bright-field and fluorescence images were obtained with a 20× objective at room temperature using a Leica DM5000 microscope (Leica Microsystems, Inc., Wetzlar, Germany) equipped with a DFC300FX camera. The images were analyzed using Leica IM1000 Version 4.0 Image Acquisition Software (Leica Microsystems, Inc.).

Statistical Analysis

Data are presented as means ± standard deviations. In figures, bar graphs represent means and error bars represent one standard deviation. A one-way analysis of variance (ANOVA) was used to look for significant differences in percentage of wound healing over time. A two-tailed Student's *t*-test was used to directly compare the extent of thermal osteonecrosis in the laser osteotomy and drill osteotomy treatment groups. A $^{*}P$-value <0.05 was considered significant.

RESULTS

Assessment of Early Histological Changes

Under SEM observation, the edges of the osteotomy defect produced by the trephine bur were rough and irregular (Fig. 1B). Formation of superficial cracks and microfractures were readily identified on the surface of the drill osteotomy defect. On the other hand, the Ti:Sapphire laser produced a defect with sharp edges and a smooth surface. No gross charring or burning of adjacent bone was observed with the Ti:Sapphire laser.

The presence of empty lacunae has been described to be indicative of osteonecrosis [35]. Histological evidence of osteonecrosis was apparent 3 days after creation of calvarial defects in both the drill osteotomy and laser osteotomy treatment groups (Fig. 2A). The bony edges of the drill osteotomy defect appeared nonviable, with a large number of empty lacunae lacking normal osteocytes. Histological staining also revealed extensive endosteal and periosteal reactions adjacent to the drill osteotomy site, which was characterized by subendosteal bone resorption and infiltration of inflammatory cells. On the other hand, the Ti:Sapphire laser ablation procedure resulted in sharp cutting edges with no microscopic irregularity of bone elements 3 days after surgery. The majority of osteocyte lacunae directly adjacent to the laser osteotomy defect contained osteocytes with normal structural characteristics (Fig. 2A).

To compare the extent of heat diffusion and associated thermal damage to surrounding tissues, the distance that empty osteocyte lacunae extended from the edge of the calvarial defect was measured in both the drill osteotomy and laser osteotomy groups at 3 days postoperatively. In the drill osteotomy group, empty osteocyte lacunae were seen to extend 699 ± 27 μm away from the edge of the defect. However, in the laser osteotomy treatment group, empty osteocyte lacunae were seen to extend 182 ± 22 μm away from the edge of the defect ($^{*}P < 0.05$; Fig. 2B).

Micro-CT Imaging Analysis

Healing after drill osteotomy was significantly delayed at 2, 4, and 6 weeks post-surgery, compared to the laser group (Fig. 3A and B). However, at 8 weeks, there was no statistically significant difference between the two groups. The mean percentage of healing was $72 \pm 8\%$ in the laser group, compared to $67 \pm 6\%$ in the drill group. Differences in healing between each time point in the laser osteotomy and drill osteotomy treatment groups, with the exception of week 8, were statistically significant ($^{*}P$-value <0.05).

Gross Findings

After 8 weeks, minimal to no adhesion or fibrosis was observed between the calvarial defect and the overlying scalp in both the laser and drill osteotomy groups. Under gross inspection, healing of defects in the laser group was slightly greater than those in the drill osteotomy treatment group. Only "peninsulas" of new bone and no islands were observed in both treatment groups, representing centripetal bone formation. New bone was firm to the touch and similar in color to surrounding calvarial bone (data not shown).

Correlation Analysis Between Radiographic and Histologic Findings

To compare the bone density in defects created by drill osteotomy to that in defects created by laser osteotomy, Movat's pentachrome (Fig. 4A) and aniline blue staining were performed. Although the bone repair process was similar in both groups at 8 weeks based on radiographic analysis, histological findings demonstrated more robust and advanced osteogenesis in defects created by laser osteotomy. In contrast to the defects created by drill osteotomy, robust trabeculated bone formation was apparent in laser osteotomy defects. Large amounts of yellow stained woven bone were appreciated throughout the defect site. On the other hand, drill osteotomy defects showed significantly less ossification ($^{*}P$-value <0.05) and formation of irregular woven bone by histomorphometric quantification of aniline blue staining (Fig. 4B).

DISCUSSION

Bone has a unique capability of undergoing spontaneous regeneration and is constantly in a state of remodeling. However, the rate and extent of bone regeneration following injury depends on multiple biological and environmental factors. It has been suggested that excessive heat production during osteotomies can impair bone regeneration [36]. Eriksson et al. [37,38] investigated the effects of heat stress on bone tissue and found that heat stress hindered osteoblast regeneration and caused bone resorption and conversion to adipocytes, thus inhibiting bone healing.

Mechanical instruments, such as oscillating saws and drills, remain the gold standard for hard tissue ablation. However, cutting of bone with mechanical instruments may cause thermal damage, bone fragmentation, and the formation of an amorphous, mineral-rich carbon layer during osteotomy [39]. In addition, traumatic vibration and biomechanical stress to adjacent bone cannot be completely excluded. Consequently, an alternative technique would be preferable to reduce the risk of induced microfractures and iatrogenic tissue trauma. Lasers offer the potential advantage of high precision and reduced collateral damage to surrounding tissues.

Various laser systems with different wavelengths, pulse durations, and repetition rates have been tested for cutting bone tissue [40,41]. Preliminary studies concentrated on the use of laser systems with wavelengths that were strongly absorbed by hard bone tissue. Since the hydroxyapatite and water found in bone tissue have very high absorption coefficients for infrared laser irradiation, holmium:YAG (Ho:YAG), Er:YAG, and CO_2 lasers appeared to be particularly suitable for osteotomies [42,43]. However, multiple reports have also shown osteotomy defects created by mid-infrared laser systems to cause delayed wound healing [44–46]. Histological analyses revealed a

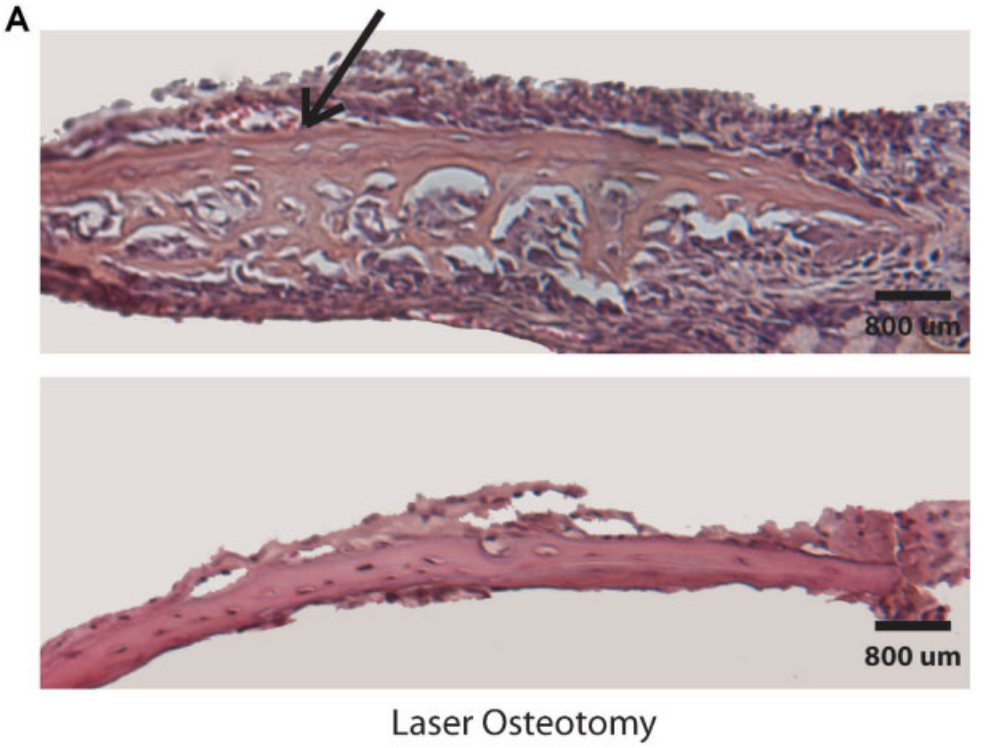

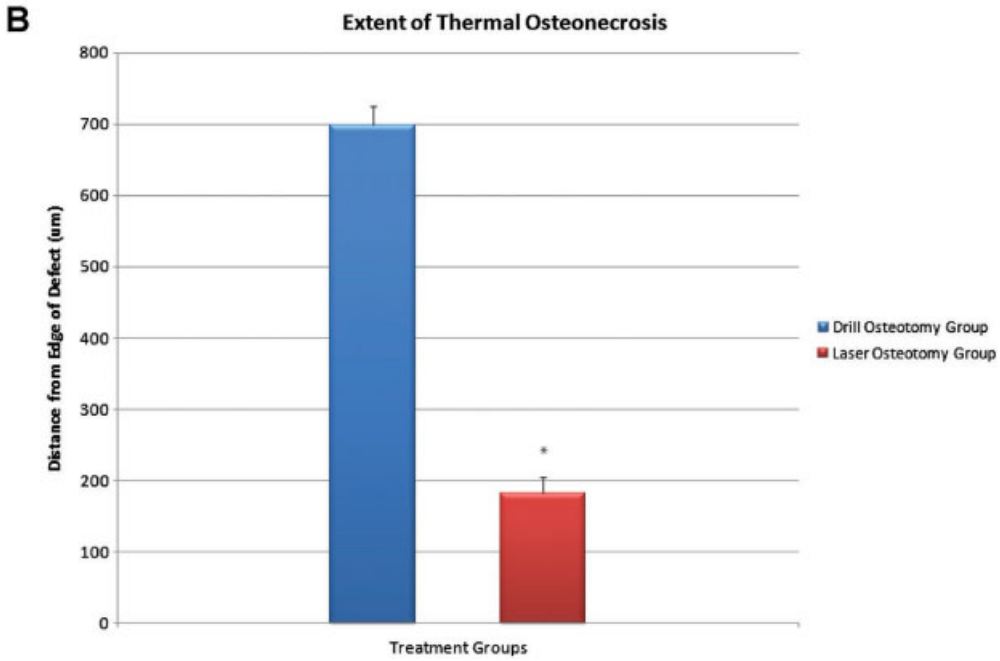

Fig. 2. **A**: Analysis of the osteotomy defects created by the trephine bur and the Ti:Sapphire laser at 3 days post-surgery by H&E staining. Marginal osteonecrosis, as evidenced by the lack of osteocytes (arrow) at the edge of the osteotomy defect, was more prominent in the drill osteotomy treatment group, scale bar represents 800 μm. **B**: The extent of osteonecrosis was delineated by measuring the distance the empty osteocyte lacunae extended from the edge of the calvarial defect ($^{*}P < 0.05$).

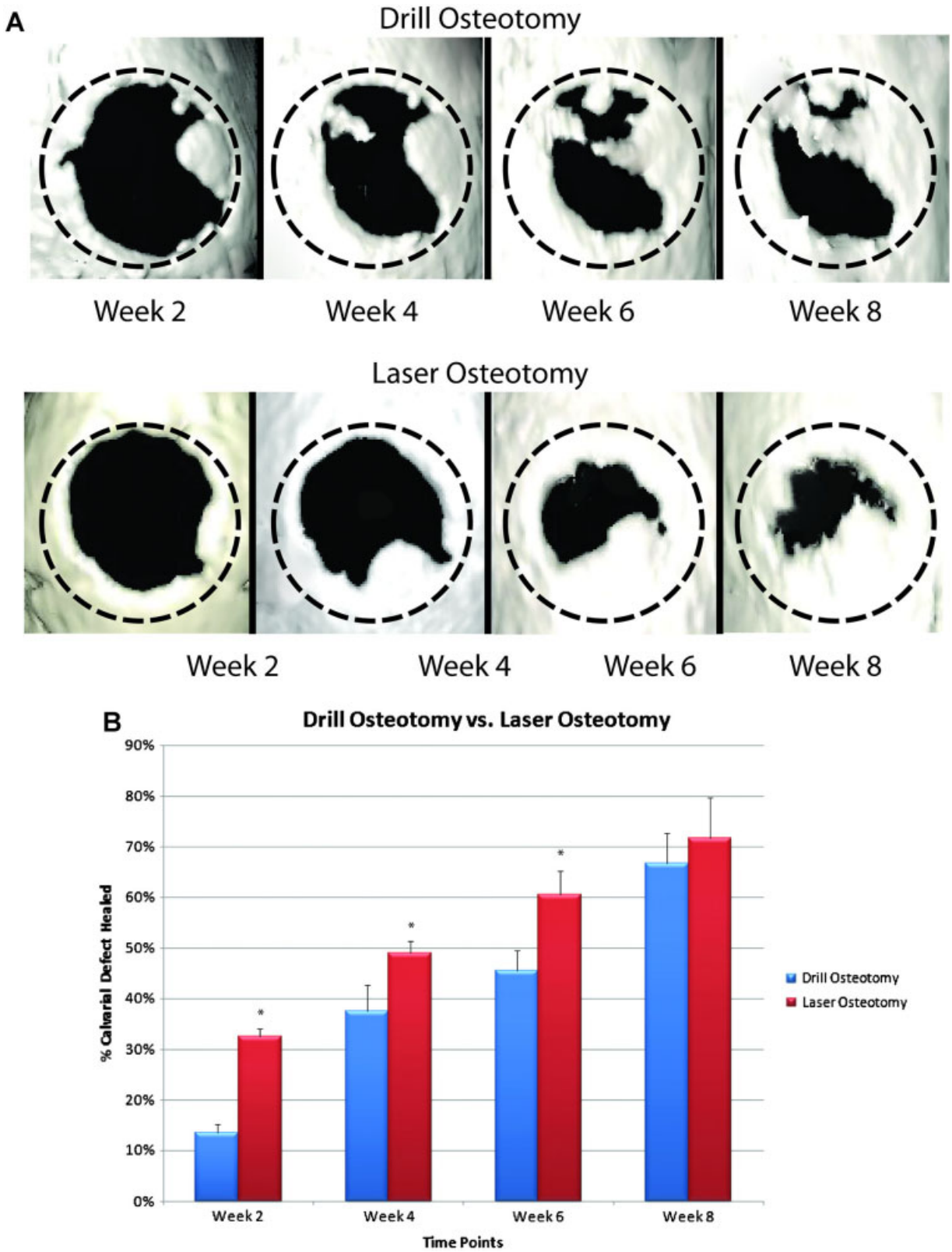

Fig. 3. **A**: Three-dimensional reconstruction of calvarial defects. Mice were scanned immediately postoperatively and at 2, 4, 6, and 8 weeks following surgery, and the residual damage zone was compared to the initial size of the ablated area. **B**: Healing of bone after laser osteotomy was significantly accelerated compared to drill osteotomy at 2, 4, and 6 weeks post-surgery ($^{*}P < 0.05$). At 8 weeks post-surgery, the mean percentage of healing in both groups were similar: 72% in the laser osteotomy group and 67% in the drill osteotomy group ($P > 0.05$).

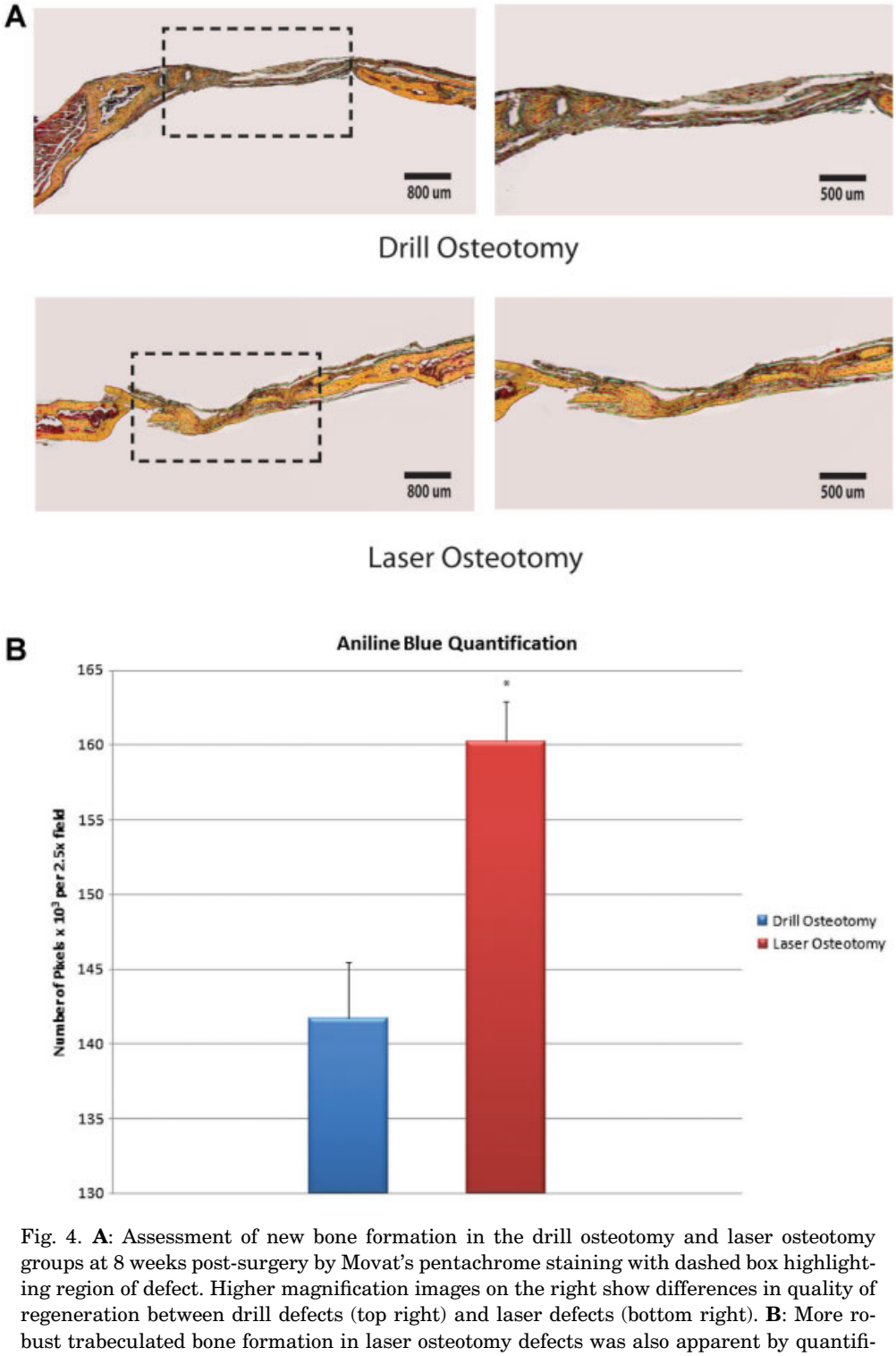

Fig. 4. **A**: Assessment of new bone formation in the drill osteotomy and laser osteotomy groups at 8 weeks post-surgery by Movat's pentachrome staining with dashed box highlighting region of defect. Higher magnification images on the right show differences in quality of regeneration between drill defects (top right) and laser defects (bottom right). **B**: More robust trabeculated bone formation in laser osteotomy defects was also apparent by quantification of aniline blue staining ($^{*}P < 0.05$).

residual carbonized layer on the treated surface due to carbonized deposit formation, thus implicating thermal damage as the major cause for delayed wound healing. On the other hand, use of short-pulse (10 microsecond) CO_2 laser has been reported to result in very limited thermal damage [47].

The introduction of femtosecond laser ablation systems may better address some of these major limitations.

McCaughey et al. [48] evaluated the ablation of ossicular bone with a femtosecond laser and found that ultra-short pulsed lasers offer a precise and efficient ablation of the stapes, with minimal thermal and negligible mechanical and acoustic damage. Liu and Niemz [49] concluded that both the ablation quantity and quality of cutting bone tissue with femtosecond laser pulses are quite close to clinical expectations required for knee joint replacement. With respect to the craniofacial skeleton, Girard et al. [50] assessed the healing of circular critical size calvarial defects of approximately 1.3 mm in diameter in mice using different wounding techniques and found that femtosecond laser cutting demonstrated an unsurpassed precision when compared to mechanical instruments. Cloutier et al. [51] compared the primary bone healing associated with femtosecond laser ablation and Er:YAG laser ablation and reported that both created wounds with healing rates similar to that of mechanical ablation. Interestingly, both of these studies observed an initial delay in healing with no statistically significant differences in healing after 12 weeks following femtosecond laser ablation. Importantly though, Girard et al. and Cloutier et al. used different laser settings and a different calvarial defect size. In addition, several groups, including ours, have demonstrated that the dura mater serves as a key regulator of calvarial regeneration [52,53]. The laser cutting systems used in the above mentioned studies were not equipped with a tissue monitoring system that shuts the laser off after perforating the bone cortex [54,55]. Thus, some damage may have occurred to the dura mater, leading to leakage of cerebrospinal fluid and delayed healing. Finally, the mice used in these experiments were far older than those used in our present study; as mice age, the ability to heal calvarial defects is lost [56]. Considering this point, it is therefore not surprising that both Girard and Cloutier noted no significant differences in bone regeneration when using the femtosecond laser, compared to mechanical drill.

In the present study, contributions from the dura mater to calvarial healing were eliminated by placing a Gore-Tex membrane between the dura mater and the parietal bone following osteotomy. This was performed to eliminate any dural contribution to healing, therefore any regeneration observed would be a result of new bone formation from the bony edge produced by the mechanical drill or laser cut. Interestingly, the drill osteotomy treatment group demonstrated slower healing that was statistically significant at weeks 2, 4, and 6. However, there was no difference observed radiographically at week 8. Of note, a recent study published by Leucht et al. [57] demonstrated that corticotomies performed with Ti:Sapphire lasers were associated with a reduced initial inflammatory response at the injury site leading to faster onset of bone healing and matrix deposition when compared to mechanical ablation. The results of the present study are in complete agreement with these findings and may have important clinical implications for osteotomies.

There are some limitations associated with the use of femtosecond lasers in surgery, most important of which are the cost and size of the laser, the beam delivery to the tissue, and the ablation rate. With the recent advent of femtosecond cataract surgery, these near-infrared ultrafast lasers have become smaller and much less expensive. While tissue removal for in the mouse model was fairly quick, application in humans would require more time due to thicker bone and large craniotomy. Nonetheless, lasers may find use in pediatric neurosurgical indications where the newly formed calvarium is thinner and more precise osteotomies are necessary. Furthermore, recent advancements with high energy femtosecond lasers allowed operating with 100–150 kHz repetition rates, which will help to alleviate some of these limitations. Finally, delivery and tight focusing of femtosecond lasers to bone requires articulated arms, much like CO_2 lasers several years ago. Though not as convenient as the optical fiber, access to the skull is not limited by such a delivery method and articulated arms have allowed wide use of CO_2 lasers in both surgery and dermatology.

To our knowledge, this is the first study to demonstrate an accelerated bone healing response after femtosecond laser ablation in a calvarial defect model with elimination of potential variability from dura mater contribution. Understanding the nature of bone regeneration in this model and optimizing bone cutting could thus greatly improve surgical outcomes following osteotomies in the craniofacial skeleton.

REFERENCES

1. Turgeon TR, Phillips W, Kantor SR, Santore RF. The role of acetabular and femoral osteotomies in reconstructive surgery of the hip: 2005 and beyond. Clin Orthop Relat Res 2005;441:188–199.
2. Sachs SA. Surgical excision with peripheral ostectomy: A definitive, yet conservative, approach to the surgical management of ameloblastoma. J Oral Maxillofac Surg 2006;64(3): 476–483.
3. Davidson SRH, James DF. Drilling in bone: Modeling heat generation and temperature distribution. J Biomech Eng Trans Asme 2003;125(3):305–314.
4. Eriksson AR, Albrektsson T. Temperature threshold levels for heat-induced bone tissue injury—A vital microscopic study in the rabbit. J Prosthet Dent 1983;50(1):101–107.
5. Stelnicki E, Heger I, Brooks CJ, Ghersi MM, Stubbs CB, Bahuleyan B, Paresi R. Endoscopic release of unicoronal craniosynostosis. J Craniofac Surg 2009;20(1):93–97.
6. Sivak-Callcott JA, Linberg JV, Patel S. Ultrasonic bone removal with the Sonopet Omni: A new instrument for orbital and lacrimal surgery. Arch Ophthalmol 2005;123(11):1595–1597.
7. Samy RN, Krishnamoorthy K, Pensak ML. Use of a novel ultrasonic surgical system for decompression of the facial nerve. Laryngoscope 2007;117(5):872–875.
8. Lustmann J, Ulmansky M, Fuxbrunner A, Lewis A. Photoacoustic injury and bone healing following 193 nm excimer laser ablation. Lasers Surg Med 1992;12(4):390–396.
9. Nelson JS, Orenstein A, Liaw LHL, Berns MW. Mid-infrared erbium-YAG laser ablation of bone—The effect of laser osteotomy on bone healing. Lasers Surg Med 1989;9(4):362–374.
10. Rayan GM, Stanfield DT, Cahill S, Kosanke SD, Kopta JA. Effects of rapid pulsed CO_2-laser beam on cortical bone in vivo. Lasers Surg Med 1992;12(6):615–620.
11. Frentzen M, Gotz W, Ivanenko M, Afilal S, Werner M, Hering P. Osteotomy with 80-μs CO_2 laser pulses—Histological results. Lasers Med Sci 2003;18(2):119–124.

12. Ivanenko M, Sader R, Afilal S, Werner M, Hartstock M, von Hanisch C, Milz S, Erhardt W, Zeilhofer HF, Hering P. In vivo animal trials with a scanning CO_2 laser osteotome. Lasers Surg Med 2005;37(2):144–148.
13. Fan K, Bell P, Fried D. Rapid and conservative ablation and modification of enamel, dentin, and alveolar bone using a high repetition rate transverse excited atmospheric pressure CO_2 laser operating at lambda = 9.3 μm. J Biomed Opt 2006;11(6):1–11.
14. Fried NM, Fried D. Comparison of Er: YAG and 9.6-μm TE CO_2 lasers for ablation of skull tissue. Lasers Surg Med 2001;28(4):335–343.
15. Li ZZ, Reinisch L, Vandemerwe WP. Bone ablation with Er-YAG and CO_2 laser—Study of acoustic and thermal effects. Lasers Surg Med 1992;12(1):79–85.
16. Peavy GM, Reinisch L, Payne JT, Venugopalan V. Comparison of cortical bone ablations by using infrared laser wavelengths 2.9 to 9.2 μm. Lasers Surg Med 1999;25(5):421–434.
17. Walsh JT, Deutsch TF. Er-YAG laser ablation of tissue—Measurement of ablation rates. Lasers Surg Med 1989;9(4): 327–337.
18. Acikgoz B, Turgut M, Ozcan OE, Ozgen T, Demirhan B, Ruacan S. Delay of cranial bone regeneration by CO_2 and Nd-YAG laser application—An experimental study related to craniosynostosis. Lasers Med Sci 1992;7(1):49–53.
19. Dela Rosa A, Sarma AV, Le CQ, Jones RS, Fried D. Peripheral thermal and mechanical damage to dentin with microsecond and sub-microsecond 9.6 μm, 2.79 μm, and 0.355 μm laser pulses. Lasers Surg Med 2004;35(3):214–228.
20. Huang H, Guo ZX. Human dermis separation via ultra-short pulsed laser plasma-mediated ablation. J Phys D Appl Phys 2009;42(16):1–9.
21. Han M, Giese G, Zickler L, Sun H, Bille JF. Mini-invasive corneal surgery and imaging with femtosecond lasers. Opt Express 2004;12(18):4275–4281.
22. Juhasz T, Frieder H, Kurtz RM, Horvath C, Bille JF, Mourou G. Corneal refractive surgery with femtosecond lasers. IEEE J Sel Top Quant Electron 1999;5(4):902–910.
23. Juhasz T, Hu XH, Turi L, Bor Z. Dynamics of shock-waves and cavitation bubbles generated by picosecond laser pulses in corneal tissue and water. Lasers Surg Med 1994;15(1): 91–98.
24. Oraevsky AA, DaSilva LB, Rubenchik AM, Feit MD, Glinsky ME, Perry MD, Mammini BM, Small W, Stuart BC. Plasma mediated ablation of biological tissues with nanosecond-to-femtosecond laser pulses: Relative role of linear and nonlinear absorption. IEEE J Sel Top Quant Electron 1996;2(4): 801–809.
25. Tsai PS, Blinder P, Migliori BJ, Neev J, Jin YS, Squier JA, Kleinfeld D. Plasma-mediated ablation: An optical tool for submicrometer surgery on neuronal and vascular systems. Curr Opin Biotechnol 2009;20(1):90–99.
26. Fischer JP, Dams J, Gotz MH, Kerker E, Loesel FH, Messer CJ, Niemz MH, Suhm N, Bille JF. Plasma-mediated ablation of brain tissue with picosecond laser pulses. Appl Phys B Lasers Opt 1994;58(6):493–499.
27. Esenaliev R, Oraevsky A, Rastegar S, Frederickson C, Motamedi M. Mechanism of dye-enhanced pulsed laser ablation of hard tissues: Implications for dentistry. IEEE J Sel Top Quant Electron 1996;2(4):836–846.
28. Neev J, DaSilva LB, Feit MD, Perry MD, Rubenchik AM, Stuart BC. Ultrashort pulse lasers for hard tissue ablation. IEEE J Sel Topn Quant Electron 1996;2(4):790–800.
29. Girard B, Yu D, Armstrong MR, Wilson BC, Clokie CML, Miller RJD. Effects of femtosecond laser irradiation on osseous tissues. Lasers Surg Med 2007;39(3):273–285.
30. Izatt JA, Sankey ND, Partovi F, Fitzmaurice M, Rava RP, Itzkan I, Feld MS. Ablation of calcified biological tissue using pulsed hydrogen-fluoride laser radiation. IEEE J Quant Electron 1990;26(12):2261–2270.
31. Kim BM, Feit MD, Rubenchik AM, Joslin EJ, Celliers PM, Eichler J, Da Silva LB. Influence of pulse duration on ultrashort laser pulse ablation of biological tissues. J Biomed Opt 2001;6(3):332–338.
32. Lustmann J, Ulmansky M, Fuxbrunner A, Lewis A. 193 nm excimer laser ablation of bone. Lasers Surg Med 1991; 11(1):51–57.
33. Ozono K, Obara M. Tailored ablation processing of advanced biomedical hydroxyapatite by femtosecond laser pulses. Appl Phys A Mater Sci Process 2003;77(2):303–306.
34. Colnot C, Thompson Z, Miclau T, Werb Z, Helms JA. Altered fracture repair in the absence of MMP9. Development 2003;130(17):4123–4133.
35. Fondi C, Franchi A. Definition of bone necrosis by the pathologist. Clin Cases Miner Bone Metab 2007;4(1):21–26.
36. Yoshida K, Uoshima K, Oda K, Maeda T. Influence of heat stress to matrix on bone formation. Clin Oral Implants Res 2009;20(8):782–790.
37. Eriksson A, Albrektsson T, Grane B, McQueen D. Thermal injury to bone. A vital-microscopic description of heat effects. Int J Oral Surg 1982;11(2):115–121.
38. Eriksson RA, Albrektsson T, Magnusson B. Assessment of bone viability after heat trauma. A histological, histochemical and vital microscopic study in the rabbit. Scand J Plast Reconstr Surg 1984;18(3):261–268.
39. Giraud JY, Villemin S, Darmana R, Cahuzac JP, Autefage A, Morucci JP. Bone cutting. Clin Phys Physiol Meas 1991; 12(1):1–19.
40. Friesen LR, Cobb CM, Rapley JW, Forgas-Brockman L, Spencer P. Laser irradiation of bone: II. Healing response following treatment by CO_2 and Nd:YAG lasers. J Periodontol 1999;70(1):75–83.
41. McDavid VG, Cobb CM, Rapley JW, Glaros AG, Spencer P. Laser irradiation of bone: III. Long-term healing following treatment by CO_2 and Nd:YAG lasers. J Periodontol 2001;72(2):174–182.
42. Buchelt M, Kutschera HP, Katterschafka T, Kiss H, Lang S, Beer R, Losert U. Erb: YAG and Hol:YAG laser osteotomy: The effect of laser ablation on bone healing. Lasers Surg Med 1994;15(4):373–381.
43. Fried NM, Fried D. Comparison of Er:YAG and 9.6-μm TE CO(2) lasers for ablation of skull tissue. Lasers Surg Med 2001;28(4):335–343.
44. Gopin BW, Cobb CM, Rapley JW, Killoy WJ. Histologic evaluation of soft tissue attachment to CO_2 laser-treated root surfaces: An in vivo study. Int J Periodontics Restorative Dent 1997;17(4):316–325.
45. Nelson JS, Orenstein A, Liaw LH, Berns MW. Mid-infrared erbium:YAG laser ablation of bone: The effect of laser osteotomy on bone healing. Lasers Surg Med 1989;9(4):362–374.
46. Nelson JS, Orenstein A, Liaw LH, Zavar RB, Gianchandani S, Berns MW. Ultraviolet 308-nm excimer laser ablation of bone: An acute and chronic study. Appl Opt 1989;28(12): 2350–2357.
47. Clayman L, Fuller T, Beckman H. Healing of continuous-wave and rapid superpulsed, carbon dioxide, laser-induced bone defects. J Oral Surg 1978;36(12):932–937.
48. McCaughey RG, Sun H, Rothholtz VS, Juhasz T, Wong BJ. Femtosecond laser ablation of the stapes. J Biomed Opt 2009;14(2):024040.
49. Liu Y, Niemz M. Ablation of femural bone with femtosecond laser pulses—A feasibility study. Lasers Med Sci 2007; 22(3):171–174.
50. Girard B, Cloutier M, Wilson DJ, Clokie CM, Miller RJ, Wilson BC. Microtomographic analysis of healing of femtosecond laser bone calvarial wounds compared to mechanical instruments in mice with and without application of BMP-7. Lasers Surg Med 2007;39(5):458–467.
51. Cloutier M, Girard B, Peel SA, Wilson D, Sandor GK, Clokie CM, Miller D. Calvarial bone wound healing: A comparison between carbide and diamond drills, Er:YAG and femtosecond lasers with or without BMP-7. Oral Surg Oral Med Oral Pathol Oral Radiol Endod 2010;110(6):720–728.
52. Behr B, Panetta NJ, Longaker MT, Quarto N. Different endogenous threshold levels of fibroblast growth factor-ligands determine the healing potential of frontal and parietal bones. Bone 2010;47(2):281–294.
53. Levi B, Nelson ER, Li S, James AW, Hyun JS, Montoro DT, Lee M, Glotzbach JP, Commons GW, Longaker MT. Dura mater stimulates human adipose-derived stromal cells to

undergo bone formation in mouse calvarial defects. Stem Cells 2011;29(8):1241–1255.
54. Rupprecht S, Tangermann K, Kessler P, Neukam FW, Wiltfang J. Er:YAG laser osteotomy directed by sensor controlled systems. J Craniomaxillofac Surg 2003;31(6):337–342.
55. Rupprecht S, Tangermann-Gerk K, Wiltfang J, Neukam FW, Schlegel A. Sensor-based laser ablation for tissue specific cutting: An experimental study. Lasers Med Sci 2004; 19(2):81–88.
56. Aalami OO, Nacamuli RP, Lenton KA, Cowan CM, Fang TD, Fong KD, Shi YY, Song HM, Sahar DE, Longaker MT. Applications of a mouse model of calvarial healing: Differences in regenerative abilities of juveniles and adults. Plast Reconstr Surg 2004;114(3):713–720.
57. Leucht P, Lam K, Kim JB, Mackanos MA, Simanovskii DM, Longaker MT, Contag CH, Schwettman HA, Helms JA. Accelerated bone repair after plasma laser corticotomies. Ann Surg 2007;246(1):140–150.